Investigations on mechanical and machinability behavior of aluminum/flyash cenosphere/Gr hybrid composites processed through compocasting

Soorya Prakash Kumarasamy [a,*], Kavimani Vijayananth [b], Titus Thankachan [b], Gopal Pudhupalayam Muthukutti [b]

[a] *Assistant professor, Department of Mechanical Engineering, Anna University Regional Campus, Coimbatore 641 046, Tamil Nadu, India*
[b] *Research scholar, Department of Mechanical Engineering, Anna University Regional Campus, Coimbatore 641 046, Tamil Nadu, India*

Abstract

This work focuses on characterization of a novel hybrid Aluminum Metal Matrix Composite (AMMC) developed through two-step compocasting method by reinforcing constant amount of flyash cenosphere (10%) and varying quantity of graphite (2%, 4% and 6%). Morphological analysis result shows the presence of dendritic arms and homogeneous distribution of the cenosphere and graphite in Al7075 matrix. The hardness and tensile strength upturn with addition of cenosphere and vice versa for the addition of graphite. The reinforcement particles have enhanced the tensile strength of Aluminum matrix from $178 \, N/mm^2$ to $213 \, N/mm^2$ as of the composite is concerned. Addition of cenosphere improves the wear resistance considerably and wear rate decreases further with graphite addition due to its self-lubricating nature. Machinability (turning) characteristics of the developed hybrid composite were studied in detail besides optimizing the machining parameters employing Artificial Neural Network (ANN) technique. Based on the ANOVA results it was found that cutting speed and % of graphite addition have the major contribution in minimizing the surface roughness of developed composite.

1. Introduction

Composites are the most successful and extensively used materials in modern industries compared with alloys or some other metals as these materials hold significantly improved mechanical properties. Tailoring the mechanical, physical and thermal properties that consist of lower density, higher specific strength, higher specific modulus, greater thermal conductivity and better abrasion and wear resistance gives advantage for metal matrix composites in their performance.

Aluminum (Al) matrix reinforced with ceramic particles has proved to be superior in its mechanical characterization when compared with its base alloy materials (Bodunrin, Alaneme, & Chown, 2015) and is most widely used for tribological parts due to their high ratio of strength to weight, stroke density and improved wear resistance (Pramanik, 2016). Particles or whiskers of Silicon Carbide (SiC), alumina (Al_2O_3) and graphite are the widely used reinforcement materials for these types of composites (Baradeswaran & Perumal, 2014; Mosleh-Shirazi, Akhlaghi, & Li, 2016). Various combinations have been tried out by researchers for hybrid composite systems with reinforcements such as SiC, Al_2O_3, rice husk ash, bamboo leaf ash, groundnut shell ash, graphite, etc. (Dinaharan, Nelson, Vijay, & Akinlabi, 2016). The performance levels derived from hybrid composite systems have been identified to be dependent on the type of reinforcements used, weight ratio of both reinforcing materials in composite, wettability between reinforcements and matrix, processing method and the metallurgical characteristics of the matrix material (Alaneme, Adewale, & Olubambi, 2014).

Among the various discontinuous reinforcements used, cenosphere a waste product during combustion of coal in thermal power plants resembling in large quantities. In addition

* Corresponding author.
E-mail address: k_soorya@yahoo.co.in (S.P. Kumarasamy).
Peer Review under the responsibility of Universidad Nacional Autónoma de México.

to lowering the cost of production, incorporation of flyash cenosphere into aluminum has proved to increase the hardness, wear resistance and stiffness with an admissible decrease in the material density.

Graphite (Gr), one of the most widely used solid lubricant materials, has enchanted many researchers to focus their investigation on development and further identify numerous applications of Al/Gr composite (Rohatgi, Ray, & Liu, 1992, Vogiatzis, Tsouknidas, Kountouras, & Skolianos, 2015). Also, researchers have recognized that Al/Gr composite exhibits superior wear properties over the base alloys due to the presence of Gr particle (Krishnan & Rohatgi, 1984; Yolshina, Muradymov, Korsun, Yakovlev, & Smirnov, 2016), which serves as a solid lubricating layer between the composite and counter surface thereby reducing the composite wear without the need for solid and liquid lubrication (Ravindran, Manisekar, Narayanasamy, & Narayanasamy, 2013).

Fabrication of AMMC is usually done by liquid casting technique or powder metallurgy route (Harrigan, 1998; Prakash, Moorthy, Gopal, & Kavimani, 2016) for the reason that these methods are typically cost effective (Kerti & Toptan, 2008). In the liquid casting technique, the particulates are mechanically well distributed over the liquid metal before casting and solidification (Moses, Dinaharan, & Sekhar, 2016). Stir casting is the cheapest and simplest method for composite material fabrication but composite materials produced through stir casting method suffers from poor incorporation and distribution of reinforcement particles in the matrix. This is especially due to the reinforcement size, which in turn results in exhibiting agglomeration tendency and reduced wettability of particles within the melt. In comparison with composites developed through stir casting method, composites produced by compocasting obtain uniform distribution of reinforcement particles in solidified matrix and also showcases better hardness with decreased porosity (Gladston, Sheriff, Dinaharan, & Selvam, 2015).

Al7075 have good fatigue strength and average machinability, but has less resistance to corrosion. Due to its remarkable high strength-to-weight ratio, this material finds a wide range of applications including aircraft fittings, worm gears, keys and various other vital components of commercial aircrafts and aerospace vehicles. It is possible to fabricate MMC by different techniques but machining plays a major role in industrial component designs like that of tolerance and dimensions; likewise the improper tool selection and machining parameter leads to poor material quality and thus increase the production cost. Whatsoever surface roughness also plays a vital role in material quality control. Depth of cut, cutting feed and spindle speed, reinforcement additions are supposed to be the major factors influencing the surface roughness of the machined surface of MMC and hence it is mandatory that all of these cutting parameter must be optimized so as to obtain material with better surface finish.

Employing optimization tools like Artificial Neural Network (ANN), Particle Swarm Optimization (PSO), Genetic Algorithm (GA) and fuzzy logic helps in attaining improved output response (Shabani & Mazahery, 2012; Shabani, Rahimipour, Tofigh, & Davami, 2015; Tofigh & Shabani, 2013). Among these, Taguchi approach is used enormously in the recent past for solving typical problems encountered in the field of optimization (Kumar & Chauhan, 2015; Shanmughasundaram & Subramanian, 2013). There are few works in which computational methods are used to optimize and predict the material properties of the newly developed materials. Mazahery and Shabani (2013) adopted stir casting technique to fabricate AMMC with varying process parameters (pouring temperature, stirring speed, stirring time, pre-heat temperature of reinforcement) and different percentage of SiC (5, 10 and 15) and results showcased that addition of SiC has improved the hardness. GA coupled PSO technique is utilized to optimize the wear parameters and to study the influence of wear parameter over wear rate; this adopted algorithm generally coincides well with the experimental values. Rahimipour, Tofigh, Mazahery, and Shabani (2014) utilized ANN coupled PSO technique to study the effect of reinforcement upon wear rate and porosity of fabricated Al–Cu based composite wherein boron carbide with different percentages are used as the reinforcements. Results stated that developed model adheres well with their experimental values.

Shabani and Mazahery (2013) developed AMMC using stir casting method. ANN technique is utilized to predict the effect of process parameter (temperature, cooling rate and reinforcement vol.%) on mechanical properties of the fabricated AMMC; a better predictably was observed by the developed model. Tofigh, Rahimipour, Shabani, and Davami (2015) fabricated alumina nanoparticle reinforced AMMC through compo casting method and also employed ANFIS coupled PSO method to obtain a optimal parameter in order to develop AMMC with uniform dispersion of reinforcement.

It is therefore proposed to undertake a study on the possibility of enhancing the mechanical properties and machinability of Al7075 alloy for worm gears production in aerospace industries. This is done by combining reinforcements (flyash cenosphere and Gr) mixed with Al7075 by two-step compocasting method. Al7075 reinforced with fixed quantity of flyash cenosphere (10 wt.%) and varying Gr (2 wt.%, 4 wt.%, 6 wt.%) is tried out in this research to form a stronger hybrid composite. Moreover it is already reported that increase in percentage of Gr beyond 7% reduces the mechanical properties of composite material (Swamy, Ramesha, Kumar, & Prakash, 2011) and hence this research aims to study the effect of Gr addition on mechanical properties by varying the weight percentage of Gr. Likewise flyash cenosphere percentage is kept constant as it is reported that 10% addition of flyash cenosphere exhibit better mechanical properties (Escalera-Lozano, Gutiérrez, Pech-Canul, & Pech-Canul, 2007). It is expedited that this novel development when put into practicality are likely to overcome the cost barrier as well as provide enhanced physical and mechanical properties as per the product requirement. A positive outcome of this research would help in commercialization of the alloy for wide range of applications in modern industries too. Also an attempt has been made to minimize the surface roughness by the way of optimizing the machining parameters through Taguchi and ANOVA techniques for turning operation of the developed composite. It

is a known fact that introduction of artificial intelligence into the field of materials has made a revolution in alloy development, process optimization, etc. This realization has made us to opt ANN in this research for predicting surface roughness of the developed composites based on varying process parameters

2. Materials and method

2.1. Materials

Commercially available Al–Zn–Mg alloy (Al7075) was selected as the matrix for composite production and its chemical composition is presented in Table 1. Al7075 is known for its excellent combination of strength and damage tolerance at elevated temperatures. With these formulation, the current study is used to improvise the corrosion resistant and wear resistance of the material by introducing suitable reinforcements viz. flyash cenosphere and Gr and thereby enrich Al7075 alloy. Besides confirming the uniformity of particle dispersions through SEM images of the sample, the average size of the flyash cenosphere particles was also identified to be in the range of 30–60 μm. The chemical composition of the flyash cenosphere is presented in Table 2.

2.2. Composites preparation

The proposed novel composite was fabricated at four different compositions as listed in Table 3, where the amount of cenosphere is kept to be constant at 10% and Gr proportion is varied from 0 to 6%. The prospective compositions of the novel composite are listed in Table 3. In addition to that 1.5 wt.% of magnesium was used as a wettability agent. Production of the composite specimens was carried out using a two-step compo casting process whose experimental setup is as shown in

Table 1
Chemical composition of Al7075.

Element	Zn	Mg	Cr	Cu	Fe	Mn	Si	Ti	Al
Wt.%	5.5	2.4	0.18	1.5	0.4	0.2	0.4	0.2	Remaining

Table 2
Chemical composition of cenosphere.

Element	SiO_2	Al_2O_3	Fe_3O_2	TiO_2	CaO	MgO	K_2O	Na_2O	H_2O
Wt.%	53	30	6	–	1	0.5	–	–	0.2

Table 3
Composition of samples.

Sample	Al7075	Flyash cenosphere	Graphite
A	100%	0%	0%
AC0Gr	90%	10%	0%
AC2Gr	88%	10%	2%
AC4Gr	86%	10%	4%
AC6Gr	84%	10%	6%

A, Al7075; C, cenosphere; Gr, graphite.

Fig. 1. Compocasting setup.

Figure 1. Al7075 rods were melted at a temperature of 690 °C. By the use of a mechanical stirrer, molten alloy was agitated to form a fine vortex and was then poured into permanent mold to fabricate the first sample of pure Al7075. Preheated flyash cenosphere particles (at a temperature of 500 °C for 60 min) were then added at a constant feed rate into the molten Al7075 in order to form the second sample. In addition to that Gr particles were added at 2, 4 and 6% level to form all of the other compositions.

To ensure uniform dispersion of reinforcement particles into the matrix alloy, two-stage stirring was employed. In the first stage, stirring was carried out for 10 min when the slurry was in a semi-solid condition at 615 °C and the second stage was carried out when the slurry was re-melted to a temperature above liquidus temperature of approximately 700 °C. The mechanical stirring process was performed at 700 rpm for 10 min and it was continued till the composite was poured into the permanent mold.

3. Results and discussion

3.1. Material depictions

3.1.1. Microstructural characterization

The scanning electron micrographs were recorded using Hitachi-S3400 scanning electron microscope (SEM). Series of grinding and polishing steps were performed on the samples surface to achieve a mirror like surface finish for micro structural examination. The samples were polished with abrasive paper of grade 600, grade 1000, and grade 1200 followed by etching using Keller's reagent (95 ml water, 2.5 ml HNO_3, 1.5 ml HCl, 1.0 ml HF) and swabbing for 10–20 s before the test.

It is observed from Figure 2(a–d) that the reinforced flyash cenosphere particles are fairly well distributed in the matrix. Presence of Gr in the matrix is clear and the same is visually evident from Figure 2(b–d). From Figure 2(a) morphology of cenosphere incorporated matrix is visualized using thermoionic emission of SEM. Micrographs taken by using secondary electron mode show cenosphere inside the Al matrix. Uniform distribution of cenosphere inside the Al matrix is confirmed from micrograph. Figure 2(b) shows the different morphological
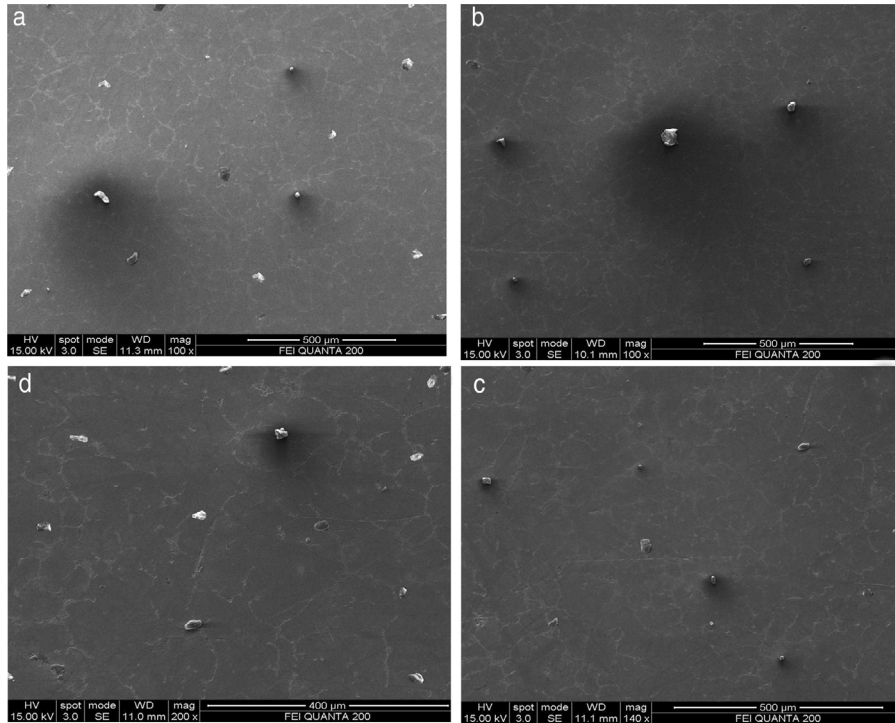
Fig. 2. SEM micrographs of (a) Al7075/10 wt.% flyash cenosphere, (b) Al7075/10 wt.% flyash cenosphere/2 wt.% graphite, (c) Al7075/10 wt.% flyash cenosphere/4 wt.% graphite and (d) Al7075/10 wt.% flyash cenosphere/6 wt.% graphite.

structure due to the impregnation of different weight percentage of Gr along with the cenosphere and aluminum matrix.

From Figure 2(c) micrograph, it can be observed that the cenosphere particles are seen in gray phase and the Gr presence is seen as dark gray phase. Further it is clearly visible and could be observed that cenosphere particles are surrounded by Gr. Figure 2(d) illustrates that surface of the samples gets smoother with the addition of Gr as experimented due to its lubricating nature.

3.1.2. Density

Density plays a vital role in the composite material study. Since Al matrix composites have bigger scope in automotive industry as well as in the space craft, they must compulsorily be light in weight. For that fact, density is usually reduced by addition of reinforcement materials of very low density and inline, from the composite samples prepared for many responsive investigations, it was observed that density decreases with such lightweight reinforcement additions. Similarly, herein decrease in density of hybrid composites was primarily due to the presence of low density flyash cenosphere particulates and it could be notified from Figure 3 that the density of composite decreases from 2.615 g/cm^3 to 2.537 g/cm^3 approximately.

3.1.3. Hardness test

Hardness tests carried out according to the ASTM E10-08 standards using Rockwell hardness tester of Model AIRAB250 with 1/16″ ball indenter and 100 kg load for 30 s was conducted at room temperature and the measurement of hardness was noted on the B scale. Tests were carried out at six different places on
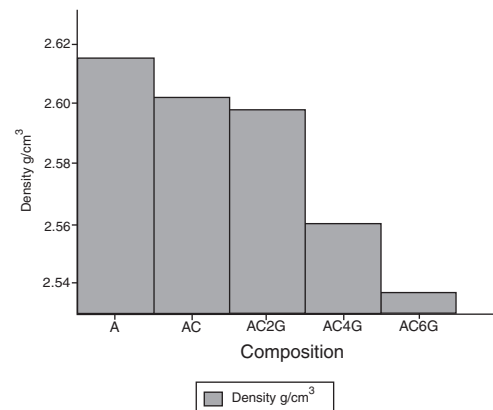

Fig. 3. Density of the developed AMMC.

each specimen and average value of hardness is notified and implied for any further usage in order to obtain precise results.

In the analysis of Al7075/flyash cenosphere/Gr hybrid composite, it was observed that hardness of the developed composite is significantly greater than that of the base alloy characterized due to the presence of cenosphere particles. The reason for increased hardness upon addition of 10% flyash cenosphere to Al7075 alloy is mainly due to the increase of ceramic reinforcement particles in the matrix. This tends for considerable increase in the surface area of reinforcement and also reduction in the matrix grain sizes. The presence of such hard surface area of particles offers more resistance to plastic deformation which leads to increase in the hardness of composites.

At the same time, hardness increases for 2% Gr addition and decreases with further addition of Gr particles to Al MMC due
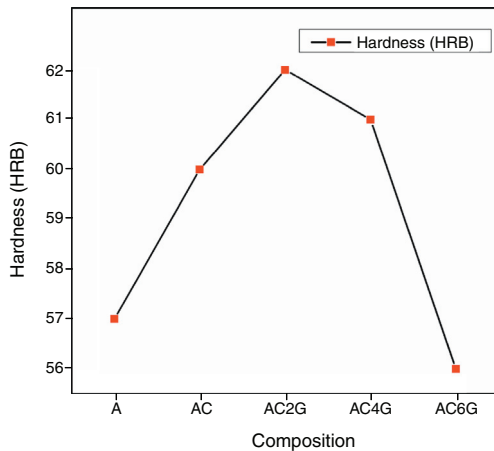
Fig. 4. Rockwell hardness of the developed AMMC.

Fig. 6. Tensile test specimens after test.

to its soft nature. From Figure 4, it is observable that there is a general decrease in hardness for any increase in weight ratio of Gr in case of hybrid composites. Hassan, Tashtoush, and Al-Khalil (2007) also stated that Rockwell hardness decrease with increase in Gr content and so it is viable to state that the present. Also, investigation is in adherence to the existing research identifications. Also, hardness value is in close adherence to the rival materials that are in existence under this category and hence it could well be augmented that the developed material is highly suitable for manufacturing gear box components.

3.1.4. Tensile test

Tensile test is majorly required because the product under consideration must withstand the tensile and compressive stress due to dynamic load acting upon the gear material.

The test specimens for tensile test were prepared with utmost care as per the dimensions mentioned in Figure 5 by using Wire Cut EDM process just because any alterations in tensile strength will obviously results in martial failure. The tensile strength was evaluated as per ASTM E08 standards using a computerized universal testing machine (TMC-Auto load master series III). In order to decrease the machining scratches and the effects of surface defects on the sample, the 1200 grid SiC grinding paper was used to polish the test samples.

Specimens after tensile test are presented in Figure 6 and it was observed that tensile strength increases with addition of flyash cenosphere content than that of Al7075 base alloy. In general, decrease in tensile strength is observed with increase in Gr content i.e., from 2 wt.% to 6 wt.% as shown in Figure 7. This fact is due to brittle nature of Gr particles which reduces
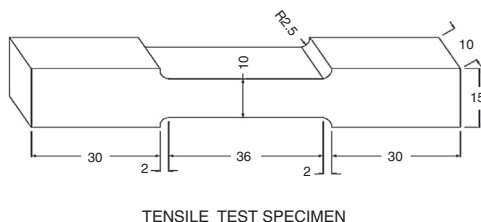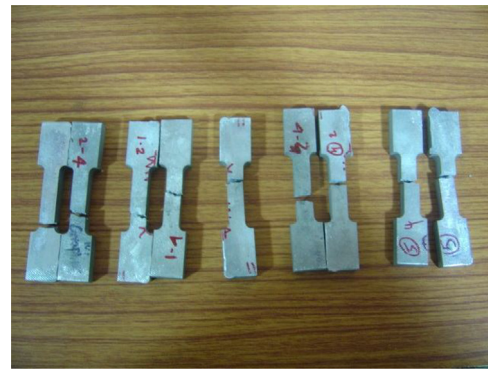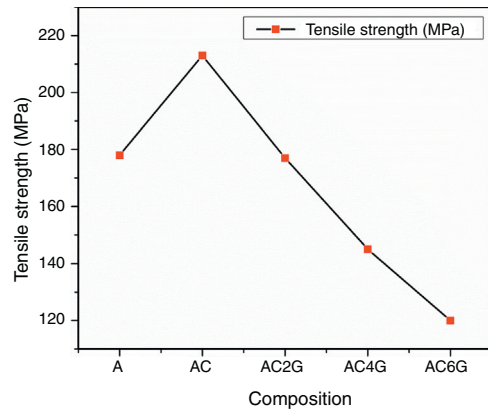

Fig. 7. Tensile strength.

the ductility of the developed MMC and thus initiates the reduction in tensile strength. Load transfer from the matrix to reinforcing particles has significantly reduced due to the presence of a greater amount of Gr and flyash cenosphere. Al matrix with dominant cenosphere particles exhibits Ultimate Tensile Strength (UTS) of 213 N/mm^2 but thereafter addition of 6% graphite lowered UTS value to approximately 120 N/mm^2 (Baradeswaran & Perumal, 2014).

3.1.5. Wear test

A DUCOM TR-20M-106 pin on disc test apparatus was used to investigate the dry sliding wear characteristics of the composites. The wear specimen of 10 mm × 10 mm × 30 mm was cut from cast samples and ends of the specimens were polished with abrasive paper of grade 600, followed by grade 1000 and finally polished using METCO Grinding/Polishing Machine. Also the sliding end of the pin on disc surface was cleaned with acetone before testing. An OHNS (Oil Hardened Nickel Steel) 55 mm diameter steel disc of 60 HRC was used as the counter surface for the real time wear test.

To fix the parameters for wear test, a soft Al alloy was used as a sample specimen. The tests done at room temperature exhibiting a relative humidity of 60–65% were made over for various loads of 20N, 40 N and 60 N at a sliding speed of 0.6, 0.8 and 1.0 m/s for a sliding distance of 1000 m, 2000 m and 3000 m. The parameters were fixed after conducting these trial and error experiments and when the sample reached a maximum wear of 2 mm.

TENSILE TEST SPECIMEN

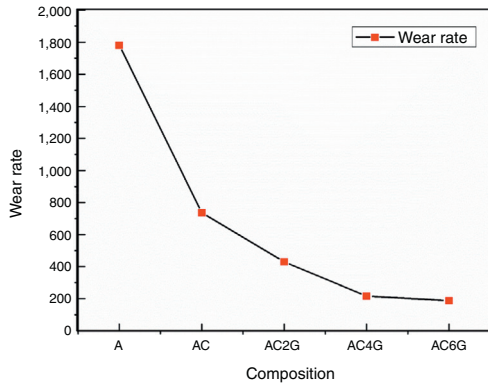Fig. 5. Dimension of tensile test specimen.

Fig. 8. Wear behavior of developed composite.

Generally lubricant is externally added to reduce the wear and it is well known that this poses several associated problems when the materials need periodic maintenance and application of lubricant particularly to wear parts which are difficult to access. In order to overcome these expeditions, in the current research a self-lubricating material viz. Gr is utilized and the same is preferred because the solid lubricant contained in them might be automatically released during sliding and thereby reduce the wear.

The wear behavior of the hybrid Al7075/flyash cenosphere/Gr composites shown in Figure 8 exhibits decremental value with the addition of flyash cenosphere and decreases even more with the addition of Gr. It reaches minimum at 10 wt.% flyash cenosphere/6 wt.% Gr and is very less than that of Al7075.

Due to the presence of flyash cenosphere particle upon the surface of matrix, the plastic deformation of matrix can be resisted and so it acts as a barrier to the movement of dislocation which causes more wear resistance than base alloy. Dropping the wear rate of hybrid composite relative to Al7075 can be reasoned to the formation of a thin lubricating Gr film on the tribosurface. The presence of Gr is reported to help in reduction of wear rate of the composites by providing a solid lubricating layer between the composite and the rubbing hard counter surface (Ravindran et al., 2013). Also it is believed that Gr particles spread at the interface between the sliding bodies and thereby decrease the coefficient of friction and hence the heat generated due to friction gets reduced to a greater extent (Basavarajappa, Chandramohan, Mukund, Ashwin, & Prabu, 2006)

SEM analysis of the worn surface of hybrid composite is as shown in Figure 9(a–d). Figure 9(a) clearly picturizes the reinforcement particles and also exhibits several damaged region caused due to high plastic deformation. Figure 9(b) reveals that a cluster of reinforcement is distributed over the matrix material wherein cenosphere is seen as gray crystal and Gr as dark crystal. From Figure 9(c) it is notable to state that these craters are formed due to the escape of cenosphere particle from the matrix material. A relatively smooth surface can be viewed from Figure 9(d) and the wear rate is low due to increased percentage of Gr and again the results are in well agreement with Baradeswaran et al. Amongst the made specimens, hybrid composite with 6 wt.% Gr content have showcased good wear resistance; because of the reason that Gr forms a thin lubricant layer and in turn reducing the wear rate; hence it can very well be claimed that the newer composite is highly suitable for gear box applications.

3.1.6. Corrosion test

Most widely used salt spray fog method was used to investigate the corrosion characteristics of the composite (ASTM
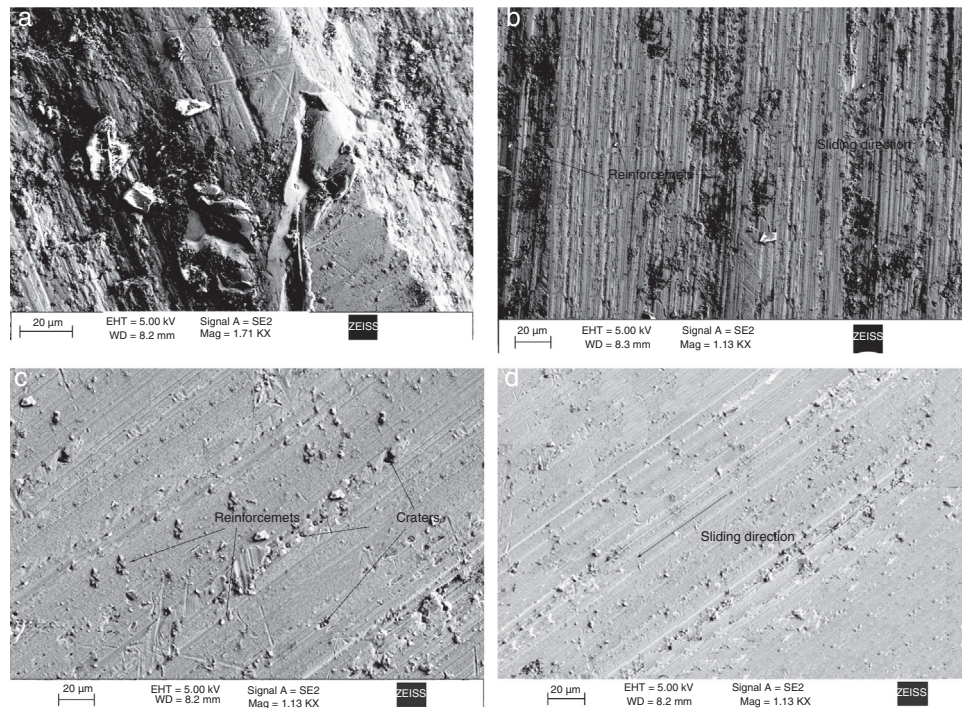

Fig. 9. SEM of worn surface of (a) Al7075 10 wt.% flyash cenosphere, (b) Al7075 10 wt.% flyash cenosphere/2 wt.% graphite, (c) Al7075 10 wt.% flyash cenosphere/4 wt.% graphite and (d) Al7075 10 wt.% flyash cenosphere/6 wt.% graphite.
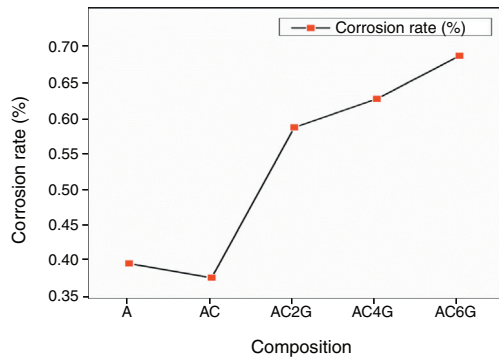
Fig. 10. Corrosion rate.

Standard B117). The test specimens were prepared by cutting the composite castings of size 45 mm × 30 mm × 5 mm and its surface were abraded using 600 grit size emery papers and are degreased. The salt solution was prepared by dissolving 5 parts by weight of sodium chloride (AR) in 95 parts of distilled water. The pH of salt solution is maintained in the range of 6.5–7.2.

Exposure zone of the salt spray chamber was maintained at a temperature of 35 ± 3 °C and specific gravity of 1.0268–1.0413. Exposure time duration for testing the specimens was set as 24 h. Specimens were dipped in clean running water to remove if there is any salt deposits on the surface and then immediately dried with a stream of clean compressed air.

The unreinforced and cenosphere reinforced alloy specimens offers better corrosion resistant compared to Gr reinforced composite specimens. This could be because of the fact that Al spontaneously forms a thin but effective oxide layer that prevents further oxidation. Growing of Al-oxide layer is noticed at the end of 24 h after test. Corrosion rate increases due to the presence of Gr and increase in its concentration raises the corrosion rate and reduces the polarization resistance of Al (Latief, Sherif, Almajid, & Junaedi, 2011).

After 19 h of duration of the test, white rust was formed on the reinforced samples followed by minor confirmation of pits. Al was pitted by sodium chloride solution and in the pit region, high

concentration of Al Chloride and hydrogen ions were present which accelerates the corrosion process in due course.

As seen in Figure 10, presence of Gr particles increases the corrosion rate since the addition of reinforcement particles causes discontinuities to the oxide film which protects the material from corrosion. Other factors influencing corrosion of the composites include porosity, isolation of alloying element to the composite interface, presence of an interfacial reaction product, with high dislocation density around the reinforcement phase and voids at the composite interface. Since these composite materials are used for gear box applications, the effect of corrosion could be minor and any further effect because of corrosion could be ignored.

Figure 11 reveals that developed hybrid composite had better mechanical properties while compared to base Al7075 alloy and hence the developed composite can be highly augmented as a better alternative to the existing Al7075 grade alloy used in aircraft's gear box. In machining, turning operation play a key role in production of parts in gear box assembly and so this work has also concentrated for machining analysis (turning operation) and performance of hybrid composite material and thereby predict the most influencing parameter of machining.

3.2. Machining characterization

3.2.1. Experimental setup

Dry turning operation was planned based on Taguchi factorial design. Minitab 16 software was used to create the design matrix and also to analyze the experimental data. Experiments are carried over casted cylindrical AMMC (AC0, AC2Gr, AC4Gr and AC6Gr) rod with 25 mm diameter. CNC turning machine was used for performing the turning operation with polycrystalline diamond (PCD) cutting tool. As per the review done over the available literatures, the machining parameters selected are graphite content (G), cutting speed (V), feed rate (F), depth cut (D) and these selected predominant parameters with 3 levels are as shown in Table 4. As surface roughness plays a key role in material quality it is chosen as the response factor. According to the design of experiment, 27 trails of
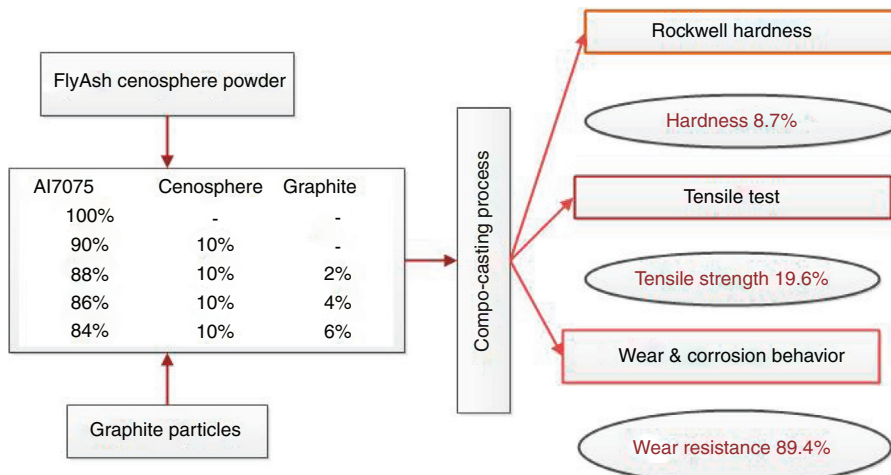

Fig. 11. Overview of mechanical characterization of hybrid composite.

Table 4
Machining parameters and their corresponding levels.

Parameters	Unit	Level 1	Level 2	Level 3
Graphite, G	wt.%	2	4	6
Cutting speed, N	mm/min	100	200	300
Feed rate, F	mm/rev	0.1	0.2	0.3
Depth of cut, D	mm	0.2	0.4	0.6

Table 5
Design of experiment for turning operation.

Sl. no.	Graphite (wt.%)	Cutting speed (mm/min)	Feed rate, F (mm/rev)	Depth of cut, D (mm)	Surface roughness, Ra (μm)
1	2	100	0.1	0.2	3.214
2	2	100	0.2	0.4	2.818
3	2	100	0.3	0.6	2.412
4	2	200	0.1	0.4	1.744
5	2	200	0.2	0.6	2.206
6	2	200	0.3	0.2	2.008
7	2	300	0.1	0.6	1.470
8	2	300	0.2	0.2	1.454
9	2	300	0.3	0.4	1.470
10	4	100	0.1	0.2	1.318
11	4	100	0.2	0.4	2.154
12	4	100	0.3	0.6	2.086
13	4	200	0.1	0.4	1.644
14	4	200	0.2	0.6	2.076
15	4	200	0.3	0.2	1.886
16	4	300	0.1	0.6	1.456
17	4	300	0.2	0.2	1.412
18	4	300	0.3	0.4	1.664
19	6	100	0.1	0.2	1.592
20	6	100	0.2	0.4	1.690
21	6	100	0.3	0.6	2.074
22	6	200	0.1	0.4	1.342
23	6	200	0.2	0.6	1.546
24	6	200	0.3	0.2	1.488
25	6	300	0.1	0.6	1.354
26	6	300	0.2	0.2	1.282
27	6	300	0.3	0.4	1.442

experiment have been conducted among which six experiments are repeated to calculate the error due to external noises. TESA RUGOSURF10 surface roughness tester is used to measure the surface roughness data at four different places of each machined component and the average value is recorded for further analyses as tabulated in Table 5.

3.2.2. Analysis of variance

Analysis of variance (ANOVA) is a method of assigning variability into identifiable sources of variation and the associated degree of freedom in an experiment. The frequency test (*F*-test) is utilized in statistics to analyze the significant effects of the parameters, which form the quality characteristics. Table 6 shows the ANOVA result of S/N ratio for surface roughness. From the analysis it is apparent that, $F_{0.05}$ value from the table is found to be 3.55 which is low when compared to the F value of Gr %, cutting speed, feed rate and depth of cut; this outcome evidence the factor that the parameters have both statistical and physical significance on the surface roughness of developed composite. From the ANOVA (Table 6), it can be observed that the Gr addition (21.9%) and cutting speed (40.8%) have contributed the major percentage on surface roughness, whereas feed rate (13.2%) and depth of cut (7.8%) have minor significance in surface finish. These results have good agreement with other similar work carried out by Shanmughasundaram and Subramanian (2013).

3.2.3. Determination of optimum factor level combination

Figure 12 shows four graphs, each of which represents the mean response and the mean S/N ratio for the Gr, feed rate, cutting speed and the depth of cut. Surface roughness increases with addition of Gr and speed but however increasing the feed rate and depth of cut decreases the surface roughness (Muthukrishnan & Davim, 2009). The values of the graphs tabulated in Table 7 are based on the S/N ratio and reveal that the optimal cutting parameters for surface roughness are $G3$, $N3$, $F1$ and $D1$.

3.2.4. Prediction of optimum performance

After selecting the optimum factor levels, prediction of the surface roughness value is done by forming regression equation as follows:

$$Ra = 2.77985 - 0.1385G - 0.00353N + 0.775556F + 0.285D$$

where Ra is the surface roughness, G is the weight percentage of Gr, N is the cutting speed and D is the depth of cut. It is very essential to perform a confirmation experiment for the parameter design, particularly when less numbers of data are utilized for optimization. The purpose of this confirmation experiment is to verify the accuracy of the developed regression model. It was observed that experimental results have good coincidence with the predicted values and falls with in the confidence limits as shown in Table 8.

Table 6
ANOVA for surface roughness.

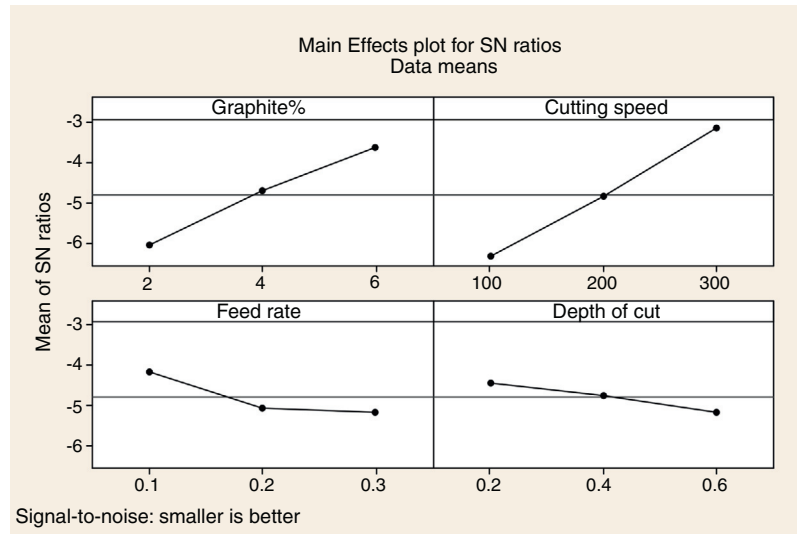| Factors	Degrees of freedom	Sum of squares	Mean square	F-test	P	Contribution (%)
Graphite, G	2	1.4084	0.7042	6.29	0.008	24
Cutting speed, N	2	2.2473	1.1236	10.04	0.001	38
Feed rate, F	2	0.1564	0.0782	0.70	0.510	3
Depth of cut, D	2	0.0614	0.0307	0.27	0.763	1
Error	18	2.0144	0.1119			34
Total	26	5.8879				

Fig. 12. Determination of optimum factors using ANOVA.

Table 7
Response table for signal to noise ratios.

Level	Graphite, G (wt.%)	Cutting speed, N (mm/min)	Feed rate, F (mm/rev)	Depth of cut, D (mm)
1	−6.054	−6.352	−4.169	−4.445
2	−4.071	−4.858	−5.070	−4.764
3	−3.633	−3.177	−5.149	−5.179
Delta	2.422	3.175	0.979	0.735
Rank	2	1	3	4

4. ANN modeling

ANN inspired from the biological neural system has emerged as a widely accepted tool in solving wide variety of problems in the field of materials and engineering. Its ability to replicate the strong learning, clustering and reasoning competence of biological neurons has made it an advanced tool in the field of expert systems. The same has been employed in many nonlinear problems due to its sound learning capability, parallel computing and non-linear mapping. A well-developed ANN model can be an effective instrument in property estimation, product design and development, optimization, predictive performance, pattern association and classification (Kara, Aslantas, & Çiçek, 2015; Padhi & Satapathy, 2013). A node is the vital element in ANN and the number of node depends on the duties and applications provided to the model. An ANN model constitutes of different number of layers comprised of varying nodes which yields outputs for the given inputs based on the training provided. These types of tools have been effectively employed in the field of material machining characteristics, tribological property estimation, mechanical property predictions, etc.

Even in this technological era, it is a known fact that surface roughness of a machined material is one of the biggest concerns while developing a material for certain other specific applications. Even though mathematical models such as regression equations can be developed for modeling the surface roughness of developed composites based on the available inputs, the predictability of the same has to be compromised; such issues can very well be reduced to a great extent just by employing ANN. In this study the ANN model is developed based on the experimental results of surface roughness obtained from Taguchi's design for experimentation and prediction of surface roughness based on the Gr quantity as reinforcement, cutting speed, feed rate and depth of cut were done thereof. At the same time it also helps in to yield sufficient understanding on the effect of process parameters over the surface roughness of developed composites.

4.1. ANN model development

Taguchi based design of experiments developed to study the surface roughness of newer Al hybrid composites along with the attained experimental results were considered for developing an ANN model to predict the surface roughness of the same for unknown values which would lay within the probabilistic distribution. The quantity of the Gr addition, cutting speed, feed rate and depth of cut, considered as the governing factors in obtaining optimal surface roughness were chosen as the inputs for developing the ANN model while the measured surface roughness was considered as the output target for training purpose. It is clearly evident from journals that back propagation training networks are considered as dominant in solving these types of problems were the ANN models are trained based on the back data. This

Table 8
Verification of optimal parameters through confirmation test.

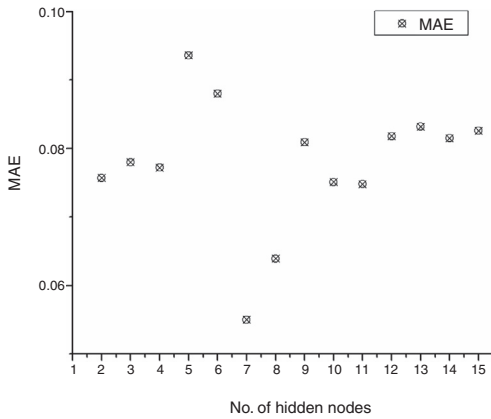| Sl. no.	Graphite (wt.%)	Cutting speed (mm/min)	Feed rate, F (mm/rev)	Depth of cut, D (mm)	Predicted, Ra (μm)	Experiment, Ra (μm)	Error %
1	6	300	0.2	0.2	1.68	1.63	2.9
2	6	350	0.2	0.2	1.58	1.54	2.5

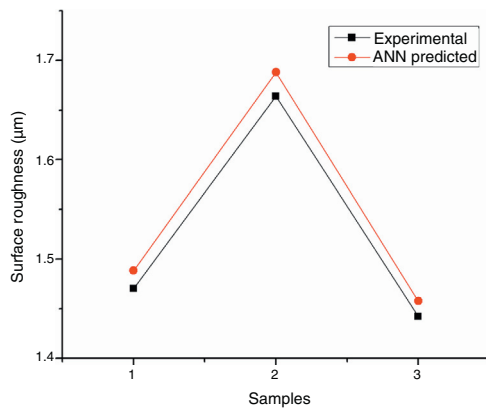Fig. 13. MAE validation of the developed models.

Fig. 14. Validated results of the model.

training algorithm works in such a manner that the error between ANN predicted values and actual values provided for training are propagated backward and the weights are adjusted accordingly after each cycle (Haque & Sudhakar, 2001).

Back propagation algorithm network models with varying hidden nodes were trained with the inputs and outputs as provided in Table 5. Out of 27 readings obtained, 24 of them are considered for training and developing the required model while the other three (Expt no. 9, 18 and 27) were employed for validating and testing the data. In MATLAB 2013, Levenberg–Marquardt back propagation based training algorithm was employed to train the back propagation network. The hidden nodes were selected and varied from 2 to 15 in a single hidden layer topology based ANN model. Literatures have proved that single hidden layer based model has the capability to solve any type of problems. Each model was trained for 1000 epochs and trained to undergo 10,000 iterations to obtain the best model. The models were evaluated based on the Mean Sum Square (MSE) value. The best model from these 10,000 models thus developed was chosen based on the least MSE value.

The models have to be validated and tested to obtain the efficient model which can predict the properties with better correlation. The Mean Absolute Value (MAE) justifies and sorts out the best developed model amongst the all. The models with varying network topology thus developed in this research along with its MAE value is provided in Figure 13.

From Figure 13 it is evident that the ANN model with single hidden layer and with 7 nodes has the least MAE value of 0.055; hence it is the best among the developed models. Thus it can be stated that a feed forward back propagation model with network topology 4-7-1 can predict surface roughness of the developed Al hybrid MMC with better efficiency.

To assure the ability of developed model, it was again tested with an unknown data (Expt no. 9, 18 and 27) that way this dataset is nowhere employed in training the model. Again from Figure 14, it is evident that the validated results are in coincidence to the yielded values and hence model hence developed has the capability to predict the surface roughness of the composite based on Gr quantity, cutting speed, feed rate and depth of cut. Figure 15 gives a clear vision of the input node, hidden
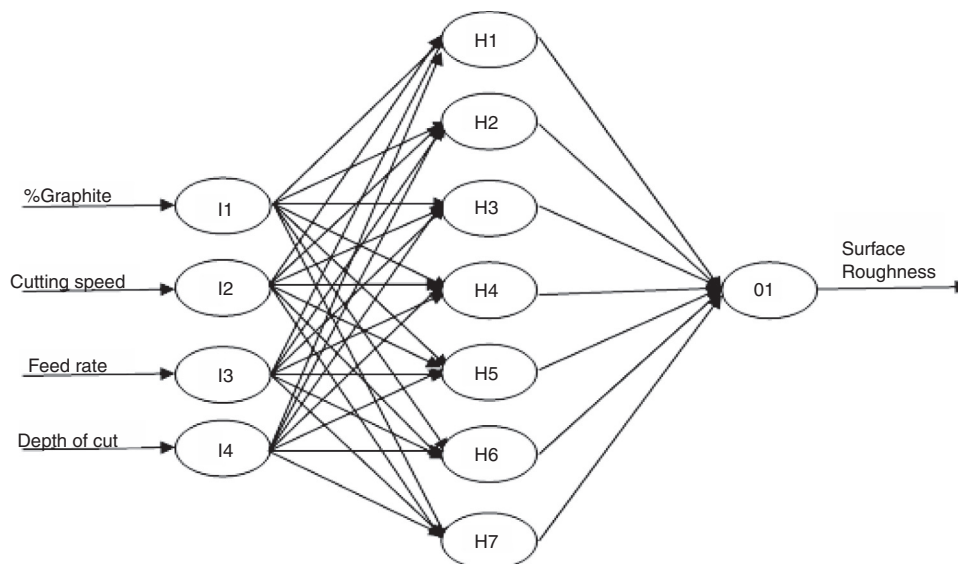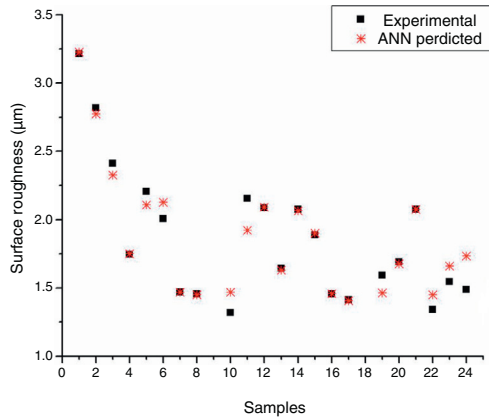

Fig. 15. ANN model with network topology 4-7-1.

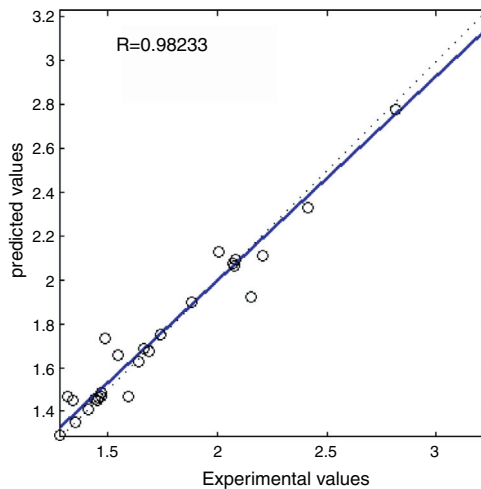Fig. 16. Validation results of trained data.

Fig. 17. Comparison between ANN and experimental values.

layer (notified with H1–H7) and output node of the developed ANN model along with the network topology.

The same ANN model was employed to predict the surface roughness of Al hybrid MMC for the given values used for training the model. The model was able to predict the surface roughness based on the given set of Gr quantity, cutting speed, feed rate and depth of cut with high efficiency and is revealed from Figure 16.

Scatter diagram, a method to validate the efficiency of the model as a linear statistical method is carried out in this research. The result which showcases the correlation created by the model between the predicted and experimental values is depicted through Figure 17.

The scatter as shown in Figure 17 showcases an *R* value of 98% which says that the model has a good predictability and the same model can be used to predict the surface of the developed composites for a given quantity of Gr, cutting speed, feed rate and depth of cut for values which lies inside the probabilistic distribution.

5. Conclusion

The Al7075–flyash cenosphere–Gr composites were produced by two-step compocasting route with different weight percentage of reinforcements (10 wt.% of flyash cenosphere and 2, 4 and 6 wt.% of Gr). Mechanical, microstructure, wear, corrosion and machinability of the developed composites were evaluated. From the study, the following conclusions are derived.

- Addition of low density flyash cenosphere particulates results in 6.8% decrement in density for the hybrid composites i.e. reduced from 2.615 g/cm^3 to 2.537 g/cm^3.
- The bulk hardness of the composites increased from 57 HRB to 62 HRB that is by 8.7% with respect to the addition of 10% flyash cenosphere and 2% Gr. On further increase in weight percentage of Gr, the bulk hardness decreases. The tensile strength of hybrid MMC is inferior due to Gr addition whereas the Al MMC without Gr exhibits better tensile strength (213 N/mm^2).
- The wear resistance of Al7075 increases with flyash cenosphere addition and even more resistance is exhibited by the Gr added hybrid MMC. Wear rate of the hybrid MMC with 10% flyash cenosphere and 6% Gr is 89.4% less than that of matrix alloy.
- Cenosphere addition decreases the corrosion rate slightly, but the corrosion rate increases vastly with increase in Gr percentage when compared with that of base alloy.
- Cutting speed and reinforcement content play a vital role in altering the surface finish of the machined composites. The developed ANN model showcased high predictability in predicting the surface roughness for the given input parameter.

Conflict of interest

The authors have no conflicts of interest to declare.

References

Alaneme, K. K., Adewale, T. M., & Olubambi, P. A. (2014). Corrosion and wear behaviour of Al–Mg–Si alloy matrix hybrid composites reinforced with rice husk ash and silicon carbide. *Journal of Materials Research and Technology*, *3*(1), 9–16. http://dx.doi.org/10.1016/j.jmrt.2013.10.008

Baradeswaran, A., & Perumal, A. E. (2014). Study on mechanical and wear properties of Al 7075/Al2O3/graphite hybrid composites. *Composites Part B: Engineering*, *56*, 464–471. http://dx.doi.org/10.1016/j.compositesb.2013.08.013

Basavarajappa, S., Chandramohan, G., Mukund, K., Ashwin, M., & Prabu, M. (2006). Dry sliding wear behavior of Al 2219/SiCp–Gr hybrid metal matrix composites. *Journal of Materials Engineering and Performance*, *15*(6), 668–674. http://dx.doi.org/10.1361/105994906X150803

Bodunrin, M. O., Alaneme, K. K., & Chown, L. H. (2015). Aluminium matrix hybrid composites: A review of reinforcement philosophies; mechanical, corrosion and tribological characteristics. *Journal of Materials Research and Technology*, *4*(4), 434–445. http://dx.doi.org/10.1016/j.jmrt.2015.05.003

Dinaharan, I., Nelson, R., Vijay, S. J., & Akinlabi, E. T. (2016). Microstructure and wear characterization of aluminum matrix composites reinforced with industrial waste fly ash particulates synthesized by friction stir processing. *Materials Characterization*, *118*, 149–158. http://dx.doi.org/10.1016/j.matchar.2016.05.017

Escalera-Lozano, R., Gutiérrez, C. A., Pech-Canul, M. A., & Pech-Canul, M. I. (2007). Corrosion characteristics of hybrid Al/SiCp/MgAl$_2$O$_4$ composites fabricated with fly ash and recycled aluminum. *Materials Characterization*, *58*(10), 953–960.

Gladston, J. A. K., Sheriff, N. M., Dinaharan, I., & Selvam, J. D. R. (2015). Production and characterization of rich husk ash particulate reinforced AA6061 aluminum alloy composites by compocasting. *Transactions of Nonferrous Metals Society of China*, *25*(3), 683–691. http://dx.doi.org/10.1016/S1003-6326(15)63653-6

Haque, M. E., & Sudhakar, K. V. (2001). ANN based prediction model for fatigue crack growth in DP steel. *Fatigue & Fracture of Engineering Materials & Structures*, *24*(1), 63–68.

Harrigan, W. C. (1998). Commercial processing of metal matrix composites. *Materials Science and Engineering A*, *244*(1), 75–79. http://www.sciencedirect.com/science/article/pii/S0921509397008289

Hassan, A. M., Tashtoush, G. M., & Al-Khalil, J. A. (2007). Effect of graphite and/or silicon carbide particles addition on the hardness and surface roughness of Al-4 wt% Mg alloy. *Journal of Composite Materials*, *41*(4), 453–465.

Kara, F., Aslantas, K., & Çiçek, A. (2015). ANN and multiple regression method-based modelling of cutting forces in orthogonal machining of AISI 316L stainless steel. *Neural Computing and Applications*, *26*(1), 237–250.

Kerti, I., & Toptan, F. (2008). Microstructural variations in cast B4C-reinforced aluminium matrix composites (AMCs). *Materials Letters*, *62*(8), 1215–1218.

Krishnan, B. P., & Rohatgi, P. K. (1984). Modification of Al–Si alloy melts containing graphite particle dispersions. *Metals Technology*, *11*(1), 41–44.

Kumar, R., & Chauhan, S. (2015). Study on surface roughness measurement for turning of Al 7075/10/SiCp and Al 7075 hybrid composites by using response surface methodology (RSM) and artificial neural networking (ANN). *Measurement*, *65*, 166–180.

Latief, F. H., Sherif, E. S. M., Almajid, A. A., & Junaedi, H. (2011). Fabrication of exfoliated graphite nanoplatelets-reinforced aluminum composites and evaluating their mechanical properties and corrosion behavior. *Journal of Analytical and Applied Pyrolysis*, *92*(2), 485–492. http://dx.doi.org/10.1016/j.jaap.2011.09.003

Mazahery, A., & Shabani, M. O. (2013). Development of the principle of simulated natural evolution in searching for a more superior solution: Proper selection of processing parameters in AMCs. *Powder Technology*, *245*, 146–155. http://dx.doi.org/10.1016/j.powtec.2013.04.035

Moses, J. J., Dinaharan, I., & Sekhar, S. J. (2016). Prediction of influence of process parameters on tensile strength of AA6061/TiC aluminum matrix composites produced using stir casting. *Transactions of Nonferrous Metals Society of China*, *26*(6), 1498–1511. http://dx.doi.org/10.1016/S1003-6326(16)64256-5

Mosleh-Shirazi, S., Akhlaghi, F., & Li, D. Y. (2016). Effect of graphite content on the wear behavior of Al/2SiC/Gr hybrid nano-composites respectively in the ambient environment and an acidic solution. *Tribology International*, *103*, 620–628.

Muthukrishnan, N., & Davim, J. P. (2009). Optimization of machining parameters of Al/SiC-MMC with ANOVA and ANN analysis. *Journal of Materials Processing Technology*, *209*(1), 225–232.

Padhi, P. K., & Satapathy, A. (2013). Analysis of sliding wear characteristics of BFS filled composites using an experimental design approach integrated with ANN. *Tribology Transactions*, *56*(5), 789–796.

Prakash, K. S., Moorthy, R. S., Gopal, P. M., & Kavimani, V. (2016). Effect of reinforcement, compact pressure and hard ceramic coating on aluminium rock dust composite performance. *International Journal of Refractory Metals and Hard Materials*, *54*, 223–229. http://dx.doi.org/10.1016/j.ijrmhm.2015.07.037

Pramanik, A. (2016). Effects of reinforcement on wear resistance of aluminum matrix composites. *Transactions of Nonferrous Metals Society of China*, *26*(2), 348–358. http://dx.doi.org/10.1016/S1003-6326(16)64125-0

Rahimipour, M. R., Tofigh, A. A., Mazahery, A., & Shabani, M. O. (2014). Strategic developments to improve the optimization performance with efficient optimum solution and produce high wear resistance aluminum–copper alloy matrix composites. *Neural Computing and Applications*, *24*(7–8), 1531–1538.

Ravindran, P., Manisekar, K., Narayanasamy, R., & Narayanasamy, P. (2013). Tribological behaviour of powder metallurgy-processed aluminium hybrid composites with the addition of graphite solid lubricant. *Ceramics International*, *39*(2), 1169–1182. http://dx.doi.org/10.1016/j.ceramint.2012.07.041

Rohatgi, P. K., Ray, S., & Liu, Y. (1992). Tribological properties of metal matrix-graphite particle composites. *International Materials Reviews*, *37*(1), 129–152. http://dx.doi.org/10.1179/imr.1992.37.1.129

Shabani, M. O., & Mazahery, A. (2012). Prediction performance of various numerical model training algorithms in solidification process of A356 matrix composites. *Indian Journal of Engineering & Materials Sciences*, *19*, 129–134.

Shabani, M. O., & Mazahery, A. (2013). The synthesis of the particulates Al matrix composites by the compocasting method. *Ceramics International*, *39*(2), 1351–1358. http://dx.doi.org/10.1016/j.ceramint.2012.07.073

Shabani, M. O., Rahimipour, M. R., Tofigh, A. A., & Davami, P. (2015). Refined microstructure of compo cast nanocomposites: The performance of combined neuro-computing, fuzzy logic and particle swarm techniques. *Neural Computing and Applications*, *26*(4), 899–909.

Shanmughasundaram, P., & Subramanian, R. (2013). Influence of graphite and machining parameters on the surface roughness of Al-fly ash/graphite hybrid composite: A Taguchi approach. *Journal of Mechanical Science and Technology*, *27*(8), 2445–2455.

Swamy, A. R. K., Ramesha, A., Kumar, G. V., & Prakash, J. N. (2011). Effect of particulate reinforcements on the mechanical properties of Al6061-WC and Al6061-Gr MMCs. *Journal of Minerals and Materials Characterization and Engineering*, *10*(12), 1141.

Tofigh, A. A., Rahimipour, M. R., Shabani, M. O., & Davami, P. (2015). Application of the combined neuro-computing, fuzzy logic and swarm intelligence for optimization of compocast nanocomposites. *Journal of Composite Materials*, *49*(13), 1653–1663.

Tofigh, A. A., & Shabani, M. O. (2013). Efficient optimum solution for high strength Al alloys matrix composites. *Ceramics International*, *39*(7), 7483–7490. http://dx.doi.org/10.1016/j.ceramint.2013.02.097

Vogiatzis, C. A., Tsouknidas, A., Kountouras, D. T., & Skolianos, S. (2015). Aluminum–ceramic cenospheres syntactic foams produced by powder metallurgy route. *Materials & Design*, *85*, 444–454.

Yolshina, L. A., Muradymov, R. V., Korsun, I. V., Yakovlev, G. A., & Smirnov, S. V. (2016). Novel aluminum-graphene and aluminum-graphite metallic composite materials: Synthesis and properties. *Journal of Alloys and Compounds*, *663*, 449–459.